ACCOUNTS of chemical research

pubs.acs.org/accounts Article

Metal Halide Superionic Conductors for All-Solid-State Batteries

Jianwen Liang, Xiaona Li, Keegan R. Adair, and Xueliang Sun*

Cite This: *Acc. Chem. Res.* 2021, 54, 1023−1033 Read Online

ACCESS | Metrics & More | Article Recommendations

CONSPECTUS: Rechargeable all-solid-state Li batteries (ASSLBs) are considered to be the next generation of electrochemical energy storage systems. The development of solid-state electrolytes (SSEs), which are key materials for ASSLBs, is therefore one of the most important subjects in modern energy storage chemistry. Various types of electrolytes such as polymer-, oxide-, and sulfide-based SSEs have been developed to date and the discovery of new superionic conductors is still ongoing. Metal-halide SSEs (Li-M-X, where M is a metal element and X is a halogen) are emerging as new candidates with a number of attractive properties and advantages such as wide electrochemical stability windows (0.36−6.71 V vs Li/Li$^+$) and better chemical stability toward cathode materials compared to other SSEs. Furthermore, some of the metal-halide SSEs (such as the Li_3InCl_6 developed by our group) can be directly synthesized at large scales in a water solvent, removing the need for special apparatus or handling in an inert atmosphere. Based on the recent advances, herein we focus on the topic of metal-halide SSEs, aiming to provide a guidance toward further development of novel halide SSEs and push them forward to meet the multiple requirements of energy storage devices.

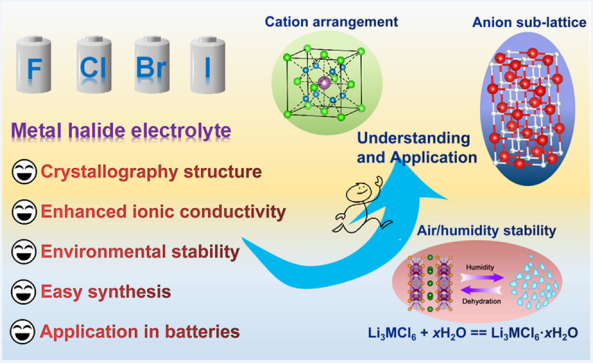

In this Account, we describe our recent progress in developing metal halide SSEs and focus on some newly reported findings based on state-of-the-art publications on this topic. A discussion on the structure of metal-halide SSEs will be first explored. Subsequently, we will illustrate the effective approaches to enhance the ionic conductivities of metal halide SSEs including the effect of anion sublattice framework, the regulation of site occupation and disorder, and defect engineering. Specifically, we demonstrated that proper structural framework, balanced Li$^+$/vacancy concentration, and reduced blocking effect can promote fast Li$^+$ migration for metal halide SSEs. Moreover, humidity stability and degradation chemistry of metal halide SSEs have been summarized for the first time. Some examples of the application of metal halide SSEs with stability toward humidity have been demonstrated. Direct synthesis of halide SSEs on cathode materials by the water-mediated route has been used to eliminate the interfacial challenges of ASSLBs and has been shown to act as an interfacial modifier for high-performance all-solid-state Li−O_2 batteries. Taken together, this Account on metal halide SSEs will provide an insightful perspective over the recent development and future research directions that can lead to advanced electrolytes.

KEY REFERENCES

- Liang, J.; Li, X.; Wang, S.; Adair, K. R.; Li, W.; Zhao, Y.; Wang, C.; Hu, Y.; Zhang, L.; Zhao, S.; Lu, S.; Huang, H.; Li, R.; Mo, Y.; Sun, X. Site-Occupation-Tuned Superionic Li_xScCl_{3+x} Halide Solid Electrolytes for All-Solid-State Batteries. *J. Am. Chem. Soc.* **2020**, *142*, 15, 7012−7022.[1] *Optimizing conditions of the Li migration mechanism to achieve the highest room-temperature ionic conductivities in metal halide-based electrolytes. The design principles including the anion sublattice, the local structure, the changing of site occupations, and order/disorder distribution of elemental/vacancies.*
- Li, X.; Liang, J.; Adair, K. R.; Li, J.; Li, W.; Zhao, F.; Hu, Y.; Sham, T.; Zhang, L.; Zhao, S.; Lu, S.; Huang, H.; Li, R.; Chen, N.; Sun, X. Origin of Superionic $Li_3Y_{1-x}In_xCl_6$ Halide Solid Electrolytes with High Humidity Tolerance. *Nano Lett.* **2020**, *20*, 4384−4392.[2] *The function of the M atom in Li_3MCl_6 was clarified to reveal the structural conversion as well as humidity tolerance mechanism.*
- Li, X.; Liang, J.; Chen, N.; Luo, J.; Adair, K. R.; Wang, C.; Banis, M. N.; Sham, T.; Zhang, L.; Zhao, S.; Lu, S.; Huang, H.; Li, R.; Sun, X. Water-Mediated Synthesis of a Superionic Halide Solid Electrolyte. *Angew. Chem.* **2019**, *131*, 16579−16584.[3] *A halide Li$^+$ superionic conductor, Li_3InCl_6, which can be synthesized in water. Most importantly, the as-synthesized Li_3InCl_6 shows a high ionic conductivity of ~2 × 10^{-3} S cm^{-1} at 25 °C.*

Received: November 15, 2020
Published: January 29, 2021

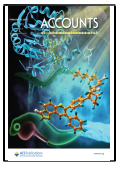

https://dx.doi.org/10.1021/acs.accounts.0c00762
Acc. Chem. Res. 2021, 54, 1023−1033

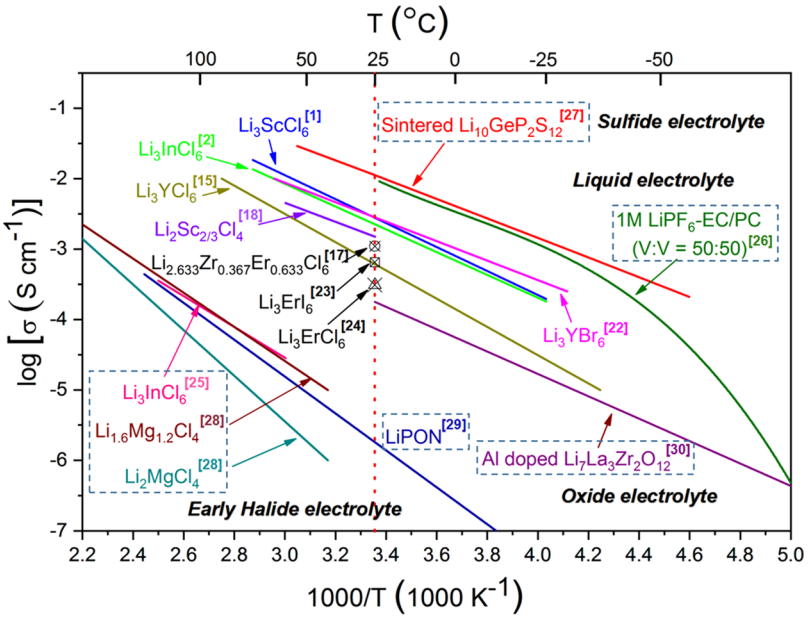

Figure 1. Evolution of ionic conductivity of the typical metal halide superionic conductors along with other lithium solid electrolytes and organic liquid electrolytes as a function of temperature.[1,2,15,17,18,22−30]

1. INTRODUCTION

The search for solid-state electrolytes (SSEs) with high ionic conductivity and good environmental/electrochemical stability is critical toward meeting the growing energy and safety demands of all-solid-state lithium batteries (ASSLBs). Over the past decades, many different classes of SSEs have been developed, such as oxide-, sulfide-, and halide-based SSEs.[4−8] Metal halides (fluoride, chloride, and bromide, *etc.*) which possess anion compounds that are more electronegative than oxide and sulfide can achieve wide thermodynamic electrochemical stability windows.[7,9] Recent findings such as room-temperature (RT) ionic conductivities over 1×10^{-3} S cm^{-1}, good stability toward oxide cathode, air/humidity tolerance, and even water-mediated synthesis routes have made the metal halide SSEs quite attractive.

In fact, metal halide SSEs have been explored for decades. Early halide SSEs ($LiAlCl_4$, Li_2MgCl_4, *etc.*),[7,10−13] which have been ignored now due to their relatively low RT ionic conductivity, played a crucial historical role in understanding the Li^+ diffusion in halide based anion frameworks. Despite the great process recently, metal halide SSEs with high ionic conductivity are still rare. There are only a few examples with the RT ionic conductivity higher than 10^{-3} S cm^{-1}, including high temperature phase Li_3InBr_6,[14] Li_3YBr_6,[15] Li_3InCl_6,[2,16] Zr doped Li_3MCl_6 (M = Y, Er),[17] $Li_3Y_{1-x}In_xCl_6$,[3] Li_xScCl_{3+x},[1] and $Li_2Sc_{2/3}Cl_4$ SSEs.[18] The ionic conductivities of the metal halide SSEs as a function of temperature are shown in Figure 1 along with other solid or organic electrolytes. Most of these metal halide SSEs with high ionic conductivity are chlorides and bromides. Fluoride-based SSEs have the widest electrochemical windows, however they still suffer from low RT ionic conductivity. Fluoride-based SSEs have only been reported in a few forms including thin film $LiAlF_4$ (1×10^{-6} S cm^{-1}),[19] bulk Li_3AlF_6 (4.4×10^{-8} S cm^{-1}),[20] thin-film $M^{II}F_2/M^{III}F_3$-doped LiF (M^{II} = Mg, Ca, Ni, Cu, Zn, Sr; M^{III} = Al, Ti, V, Cr, Ga, Y, Ce)[21] with the highest ionic conductivity reaching 5×10^{-7} S cm^{-1}. Upon doping, the RT ionic conductivity can be improved by 1 order of magnitude, which is still not high enough to achieve acceptable ASSLBs. It still needs to pay more attention to develop the new fluoride electrolyte with higher ionic conductivity. In addition, most fluorides are toxic which also restricts their further development.

In this Account, we will focus on the Li-M-X component, where M is Sc, Y, Ln, and In; and X is a halogen. We will discuss the work conducted by our group on the development of Li-M-X SSEs in the past few years: (i) our work associated with an understanding of the structure, Li^+ transport mechanisms, and effective approaches to enhance ionic conductivity; (ii) our findings on revealing the complex physical phenomenon of Li^+ transport and the related factors, including anion sublattice framework, cation order−disorder effects, Li^+ carrier concentration, and vacancy concentration for Li^+ diffusion as well as cation blocking effects, *etc*; (iii) the design of metal-halide electrolytes with improved environmental stability; and (iv) the humidity tolerance and water-mediated synthesis process of Li_3InCl_6 electrolyte. Taken together, this Account on Li-M-X SSEs will provide an insightful perspective over the recent development and future research directions of advanced metal halide SSEs for the field of ASSLBs.

2. RATIONAL DESIGN FOR SUPERIONIC CONDUCTORS

2.1. Crystallography

The stacking structure of metal halide Li-M-X ionic crystals requires ions of different radius to be arranged based on their electrostatic forces. Thus, the structure of Li-M-X is highly dependent on the radius, polarity, and arrangement of ions. The ionic radii of F^- (122 pm), Cl^- (167 pm), Br^- (182 pm), and I^- (202 pm) is larger than that of Li^+ (73 pm in tetrahedron, 90 pm in octahedron) and metal ions M^{3+} (88−118 pm). Therefore, the structural framework of these metal halide electrolytes is built up by the anion stack sublattice and influenced by the volume and polarity of the cation species. It should be noted that all of the ionic radii in this paper are

https://dx.doi.org/10.1021/acs.accounts.0c00762
Acc. Chem. Res. 2021, 54, 1023−1033

Table 1. Polarizability and Ionic Radii of Cations and Anions of Metal Halide SSEs

ion	Li^+	In^{3+}	Sc^{3+}	Y^{3+}	Er^{3+}	$La^{3+} \sim Lu^{3+}$	F^-	Cl^-	Br^-	I^-	O^{2-}	S^{2-}
coordination number	6	6	6	6	6	6	6	6	6	6	6	6
polarizability α, (Å^3)	0.03	0.51	0.286	0.55	0.69	~1.14−0.606	1.04	3.66	4.77	7.10	3.88	10.2
Pauling radius (pm)	76	80	74.5	90	89	~103.2−86.1	136	181	195	216	140	184
crystal radius[a] (pm)	90	94	88.5	104	103	~117.2−100.1	122	167	181	202	124	170
$t_{M/F}$	0.74	0.77	0.73	0.85	0.84	~0.96−0.82						
$t_{M/Cl}$	0.54	0.56	0.53	0.62	0.62	~0.62−0.60						
$t_{M/Br}$	0.50	0.52	0.49	0.57	0.57	~0.57−0.55						
$t_{M/I}$	0.45	0.47	0.44	0.51	0.51	~0.51−0.50						

[a]Crystal radius original from R. D. Shannon's research.[31]

Shannon's radius.[31] Based on the law of ionic packing, the structure is stable only when the cation and anion are in close contact. The radius ratio of cation to anion (r^+/r^-), marked as t, must meet certain conditions. For example, when t is range from 0.732 to 1, the cation will fill in the interstitial site of the cubic structure made up of 8 anions to form an MX_8 cube, which is similar to the CsCl structure. When the radius of the cation is reduced and t is between 0.414 and 0.732, the cation will occupy the octahedral site of six anions and then a MX_6 octahedron structure will be formed. When a smaller cation cannot fully fill the octahedron site, the structure will change to a more stable MX_4 tetrahedron structure (t = 0.255−0.414) or a MX_3 triangle structure (t = 0.155−0.255). Table 1 reveals the ionic radius of cations and anions of typical Li-M-X composition and the radius ratio of M cation to X anion ($t_{M/X}$). For fluoride, the $t_{M/F}$ value is higher than 0.732 for most compositions. Thus, the Li-M-F structures tend to form a $LiMF_4$ phase with M ion occupancy in the cubic site of the F^- framework (MF_8 cube). All values of the $t_{M/X}$ (X is Cl, Br, I) as well as $t_{Sc/F}$ are between 0.414 and 0.732, resulting in a stable Li_3MX_6 phase with the same local anion coordination environment of MX_6 octahedron. However, until recently, there have only been a few examples of Li_3MX_6 phase found in the inorganic crystal structure database.[7] There are many Li-M-X compounds, especially for iodides, that have not been synthesized. For example, for chloride compounds, there is no report of any kind of Li-Ln-Cl phase when the Ln ion radius is higher than 108.7 pm (La^{3+}, Ce^{3+}, Pr^{3+}, Nd^{3+}, Pm^{3+}, Sm^{3+}, Eu^{3+}). For bromide compounds, there are no Li-Ln-Br phases that have been reported when the Ln ion radius is higher than 111 pm (La^{3+}, Ce^{3+}, Pr^{3+}, Nd^{3+}, Pm^{3+}). At the same time, only two kinds of Li-M-I materials (Li_3ScI_6, Li_3ErI_6) have been found to date. Whether the lack of Li-M-X components is an intrinsic thermodynamic result or due to difficult synthesis processes remains unclear.

In the ternary chlorides of Li_3MCl_6, there are two kinds of Cl^- sublattice structures, including cubic close packing (ccp) and hexagonal close packing (hcp),[7] which can be further divided into three phase structures. The first is a trigonal structure ($P\bar{3}m1$) with hcp anion sublattice (hcp-T). The second is an orthorhombic structure (*Pnma*) with hcp anion sublattice (hcp-O). The difference between the hcp-O and hcp-T crystal structures is the same ABAB stacking of close-packed Cl^- with different symmetrical arrangements of Li^+ and M^{3+} in the octahedral sites. The last is monoclinic structure with an ABCABC stacking of the ccp anion sublattice (ccp-M). Typically, when the radius of M^{3+} ranges from 106.3 pm (Tb^{3+}) to 102 pm (Tm^{3+}), the Li_3MCl_6 can maintain the hcp-T structure. In this case, $t_{M/Cl}$ ranges from 0.611 to 0.637. Moreover, when the radius of M^{3+} is smaller than 102 and larger than 100 pm (Yb^{3+} and Lu^{3+}), the structure of Li_3MCl_6 converts to the hcp-O structure. In this case, $t_{M/Cl}$ ranges from 0.599 to 0.611. When further reducing the radii of M^{3+}, the structure will convert from an hcp to ccp anion sublattice such as Li_3ScCl_6 ($t_{Sc/Cl}$ = 0.530) and Li_3InCl_6 ($t_{In/Cl}$ = 0.563). Different to chloride-based ternary halides, all of the Li_3MBr_6 and Li_3MI_6 reveal the same ccp-M structure.[7] Although only a few systems with high ionic conductivity have been reported, it can be inferred that there will be a large number of potential components with high ionic conductivity. Furthermore, very limited doping or substitution studies on the aforementioned metal-halide SSEs can be found. It is quite possible to further enhance the ionic conductivity and electrochemical performance of the Li-M-X electrolytes.

2.2. Li Ion Transport Kinetics

Li ion transport kinetics are the key factor in developing SSEs. In fact, the hopping motion of Li^+ is a universal feature of Li^+ transport in SSEs. The crystal lattice restricts the positions and the conducting paths of Li^+. For Li-M-X SSEs with a ccp-M structure,[9,15] the pathways of Li^+ conduction are connected via tetrahedral interstitial sites between edge-sharing octahedral sites in all three directions, forming a three-direction isotropic diffusion network. For the hcp anion arrangement (hcp-O and hcp-T),[9] Li^+ transports along the *ab*-plane are via tetrahedral interstitial sites, which is similar to the ccp-M structure. Along the *c*-axis, the diffusion paths are directly connected between neighboring octahedral sites. Other than the long-range crystal lattice structure, local order−disorder of Li^+ sublattices and distortion of the local structure also play a crucial role in the Li^+ transport process. It should be noted that the order−disorder of the Li^+ sublattice and distortion of the local structure often appear together due to defects. Other crystallographic and electronic factors also affect the Li^+ transport kinetics, such as the polarity of ion induced lattice dynamics and the proximity of metal ions to activate or block Li^+ hopping. These transport phenomena will be discussed in the following sections and have strong effects on the Li^+ mobility in metal halide SSEs.

2.3. Defect Chemistry

Different from the long-range structural characteristics, defects always induce the local structure distortions or short-range arrangement.[32] An attractive feature of solid-state structures is the possibility of turning defect-chemistry to determine the effectiveness of the Li^+ hopping in the lattice. The Li^+ hopping process is sensitive to the active Li^+ and vacancy concentration, which can lead to orders of magnitude change in conductivity. The ion conduction through vacancies is the dominant mechanism for the diffusion of Li^+ in many kinds of superionic conductors.[33] Figure 2 reveals the important crystal structures

https://dx.doi.org/10.1021/acs.accounts.0c00762
Acc. Chem. Res. 2021, 54, 1023−1033

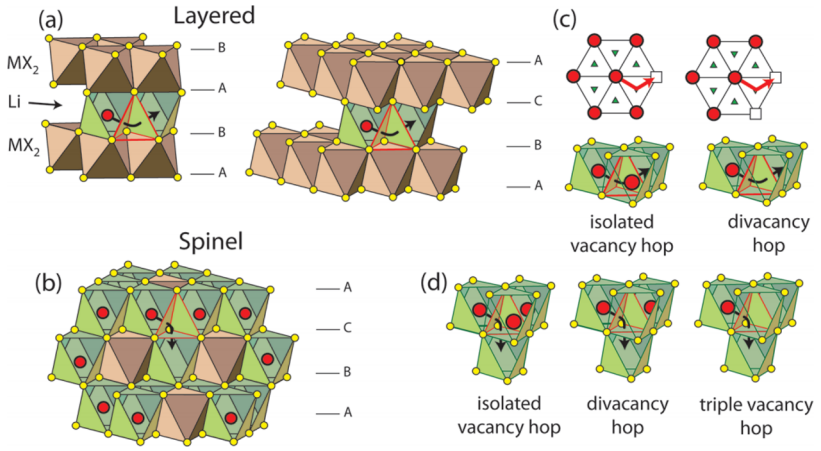

Figure 2. Important crystal structures and Li hopping mechanisms in metal halide superionic conductors based on vacancy cluster. (a) Layered structure (with hcp or ccp anion sublattice) and (b) spinel structure. (c,d) Diffusion in these structures by vacancy clusters (divacancies in the layered form and triple and divacancies in the spinel form). Red is Li, yellow is Cl. Panels a–d reproduced with permission from ref 33. Copyright 2013 American Chemical Society.

and Li^+ hopping mechanisms induced by vacancy clusters in Li-M-X systems. Compared to the constriction against the direct or ring exchange diffusion process, the energy barrier of Li^+ diffusion based on the vacancy mechanism in the close-packed lattice is much smaller. The structure of Li_3MX_6 is essentially a distorted rock-salt LiX structure, which can be considered as M^{3+} doping in LiX.[16] Particularly, one M^{3+} doping will remove three Li^+ cations and introduce two vacancies in the octahedral interstitial sites. As a result, the vacancies occupy ~33.3% octahedral interstitial sites in the structure of Li_3MX_6 and the ratio of Li^+, M^{3+}, and vacancies is 3:1:2. Presumably, these vacancies originate from aliovalent M^{3+} cation doping of Li^+ and are essential to the high ionic conductivity of the crystalline Li_3MX_6 structures such as Li_3InCl_6, Li_3ScCl_6, and Li_3YBr_6, *etc.* Vacancy clusters, grouping of vacancies within the crystal lattice and defect chemistry, serve as important parameters for Li^+ transport in these vacancy-rich environments.

Further aliovalent substitution or doping of metal ions to optimize vacancies as well as Li^+ concentration in a mobile Li^+ sublattice is an effective strategy to improve the ionic conductivity of inorganic materials. Nazar et al. reported $Li_{3-x}M_{1-x}Zr_xCl_6$ (M = Y, Er) SSEs with RT ionic conductivity up to 1.4×10^{-3} S cm^{-1} by using the aliovalent substitution strategies.[17] The substitution of M^{3+} by Zr^{4+} can introduce a large number of vacancies. Meanwhile, the lattice structure will be affected by the radius of different metal cations in the metal halide electrolyte. The substitution of M^{3+} ion by a smaller radius Zr^{4+} ion is accompanied by an hcp-T to hcp-O transition. Moreover, isovalent substitution is another strategy for improving the ionic conductivity. Although the isovalent substitution of metal ions cannot induce vacancy or Li content, it can distort the local structure or even affect the anion stacked sublattice based on different radii and polarizability of the introduced cation. Our group reported a series of $Li_3Y_{1-x}In_xCl_6$ ($0 \le x < 1$) materials by using a smaller ion of In^{3+} to substitute the Y^{3+} cation in the Li_3YCl_6 SSE.[3] When increasing the In^{3+} content, the structure is gradually converted from hcp-T to hcp-O and then to the ccp-M. The $Li_3Y_{1-x}In_xCl_6$ ($0 \le x < 1$) SSEs with the ccp anion sublattice revealing more than 10 times higher Li^+ conductivity when compared to those with an hcp anion sublattice. Afterward, Mo et al. performed a systematic study on the known Li-containing chlorides superionic conductor and their doped effect based on first-principles computation,[34] and they predicted many potential compounds with high Li-ion conductivities. Furthermore, they found that the Li-ion migration is greatly impacted by the cation configuration and concentrations. As a result, a low Li octahedral occupancy (≈40–60%), low cation concentration, and sparse cation distribution can increase the Li-ion conduction in chlorides.

2.4. Lattice Dynamics

Lattice dynamics describe the atomic vibrations in crystal structures, which can affect the diffusion of ions.[35−38] In fact, greater Li^+ mobility is correlated with decreasing lithium vibration frequency. When analyzing the relationship between ionic transport and the polarizability of the lattice, the phonon properties, *etc.*, it can be confirmed that the polarizability of the host ion lattice affects the lattice vibration strength and the Li^+ mobility kinetics by changing the activation barrier and prefactor of the Arrhenius equation.[39] Wakamura et al.[40] revealed that low activation energies of Li^+ transport are correlated with "low-energy" phonon frequencies and the high-frequency dielectric constant. Thus, a softer, more polarizable anion sublattice is beneficial for ionic transport. Table 1 reveals the polarizability of cation and anion of typical Li-M-X electrolytes. The polarizability and ionic radius of O^{2-} and S^{2-} are also shown for comparison. It can be found that the halogen anion with the lowest polarizability is F^-, which is less than one-third of Cl^-. Thus, in all of the halide SSEs, fluorides reveal the lowest ionic conductivity. So far, no fluoride SSEs with RT ionic conductivity higher than 1×10^{-5} S cm^{-1} has been discovered. The polarizability of Cl^- is similar to O^{2-} and much lower than S^{2-}. Thus, the lattice vibration strength of a Cl^- sublattice is similar to the O^{2-} sublattice, and some chlorides exhibit high ionic conductivity. At the same time, bromide and iodide have higher polarizability than chloride, which suggests that they can achieve a faster Li^+ migration. For example, Li_3YBr_6 has a higher RT ionic conductivity than Li_3YCl_6 (3×10^{-3} S cm^{-1} for Li_3YBr_6 vs 5.1×10^{-4} S cm^{-1} of Li_3YCl_6).[15,22] Li_3ErI_6 also has a higher RT ionic conductivity when compared to Li_3ErCl_6 (6.5×10^{-4} S cm^{-1} for Li_3ErI_6 vs 3.3×10^{-4} S cm^{-1} of Li_3ErCl_6).[23] Although sulfides and iodides have softer lattices than chlorides and possess higher

https://dx.doi.org/10.1021/acs.accounts.0c00762
Acc. Chem. Res. 2021, 54, 1023−1033

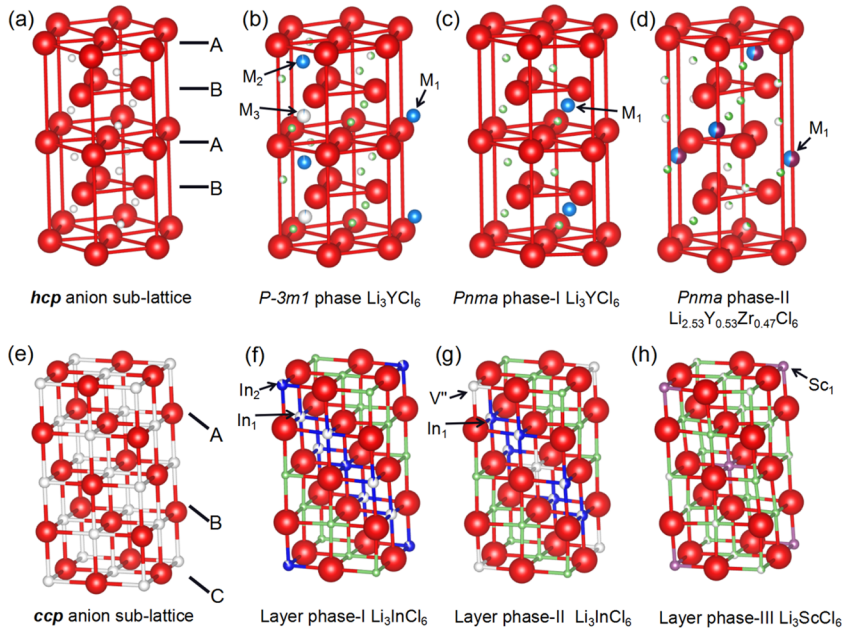

Figure 3. Metal-halide structures based on the anion sublattice framework: (a) hcp anion sublattice framework, (b) trigonal structure of Li_3YCl_6, (c) orthorhombic structure of Li_3YCl_6, (d) orthorhombic structure of $Li_{2.53}Y_{0.53}Zr_{0.47}Cl_6$, (e) ccp anion sublattice framework, (f–h) layer structure of Li_3InCl_6, Li_3InCl_6 based on the water-synthesized process and Li_3ScCl_6. Red is Cl, white is vacancy, and green is Li.

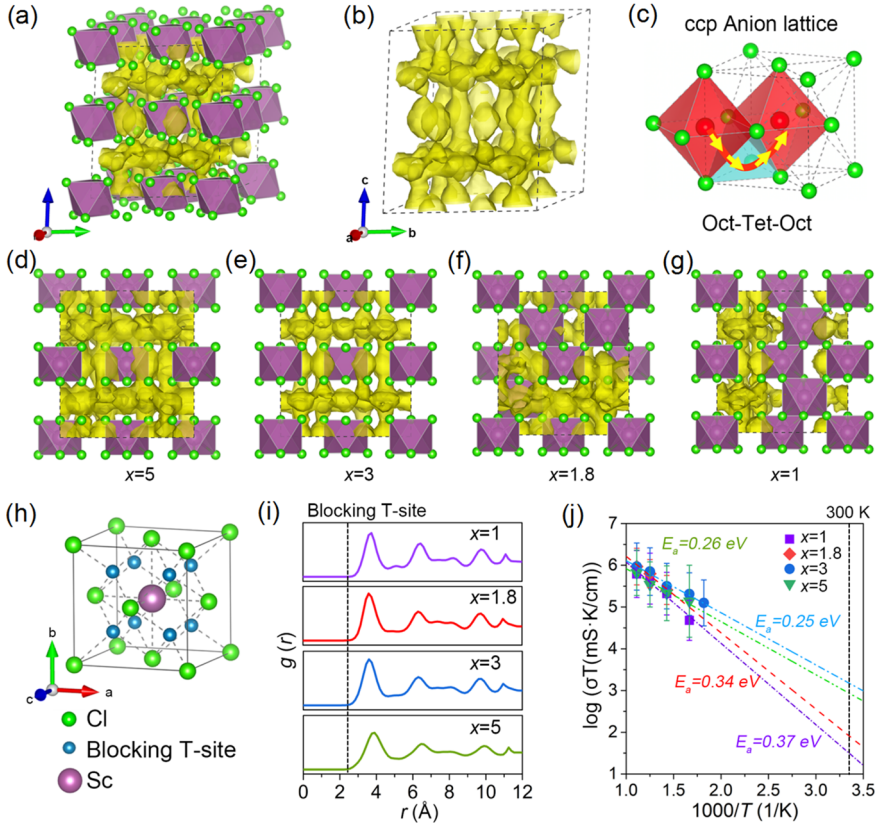

Figure 4. Diffusion mechanism of the Li_xScCl_{3+x} SSEs: (a, b) Li^+ probability density marked by yellow isosurfaces; (c) Li^+ migration pathways in ccp-anion stacking sublattice of Li_3ScCl_6 structure; (d–g) Li^+ probability density of (d) Li_5ScCl_8 (x = 5), (e) Li_3ScCl_6 (x = 3), (f) $Li_{1.8}ScCl_{4.8}$ (x = 1.8), and (g) $LiScCl_4$ (x = 1) structures; (h, i) blocking effect of Sc^{3+} in Li^+ diffusion; and (j) Arrhenius plot of Li^+ diffusivity in Li_xScCl_{3+x} (x = 1, 1.8, 3, and 5) from simulations. Panels a–j are reproduced with permission from ref 1. Copyright 2020 American Chemical Society.

ionic conductivity, their stability against electrochemical oxidation is much lower than chlorides and fluorides.[9,41] Modifying the lattice dynamics will be an emerging strategy for the discovery of new ionic conductors, however a trade-off between enhanced conductivity and electrochemical stability should be considered. The structural framework built by

https://dx.doi.org/10.1021/acs.accounts.0c00762
Acc. Chem. Res. 2021, 54, 1023−1033

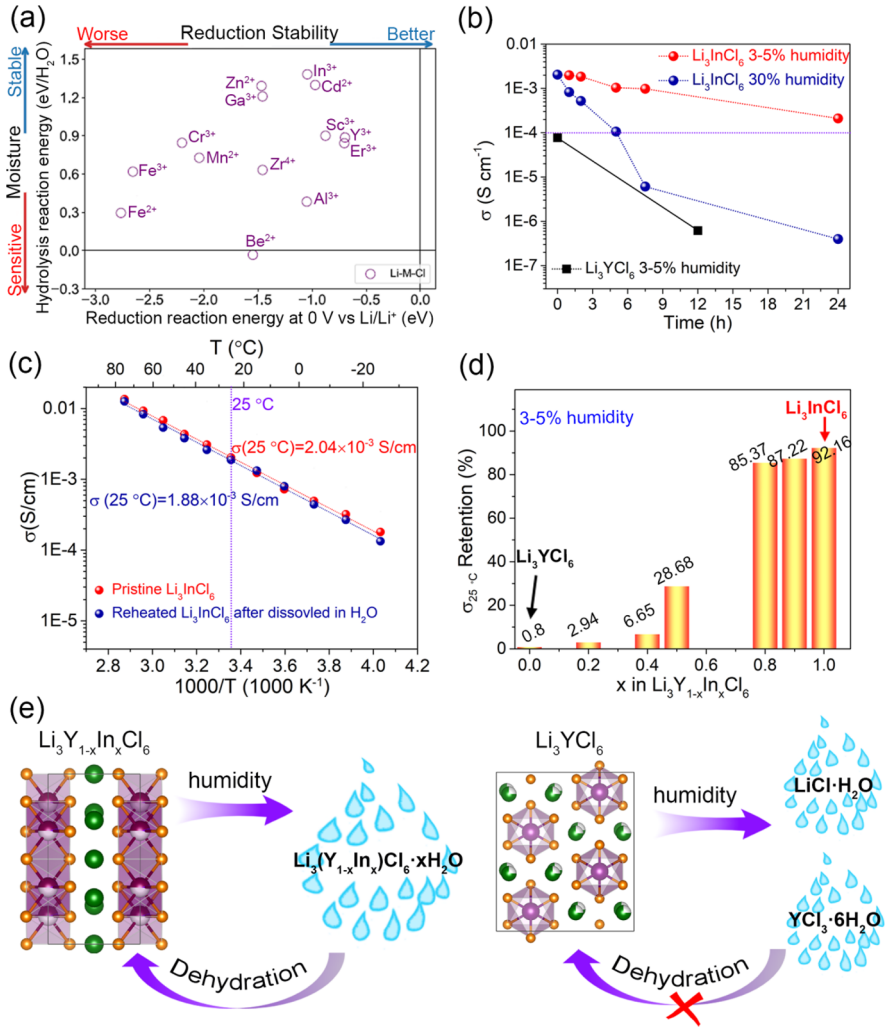

Figure 5. (a) Moisture stability versus reduction stability for Li-M-Cl, (b) ionic conductivity evolution of Li_3InCl_6 and Li_3YCl_6 exposed to humidity, (c) ionic conductivities of the pristine Li_3InCl_6 and the reheated Li_3InCl_6 after dissolving in water, (d) comparison of the ionic conductivity retention of $Li_3Y_{1-x}In_xCl_6$ SSEs before and after exposure to air with 3−5% humidity for 12 h followed by a reheating process, and (e) schematic illustration of the humidity stabilities of $Li_3Y_{1-x}In_xCl_6$ and Li_3YCl_6. Panel a is reproduced with permission from ref 43. Copyright 2020 John Wiley & Sons, Inc. Panels b and c are reproduced with permission from ref 2. Copyright 2019 John Wiley & Sons, Inc. Panels d and e are reproduced with permission from ref 3. Copyright 2020 American Chemical Society.

multiple anions such as Li-M-Cl-F, Li-M-Cl-O, and Li-M-Cl-Br, which can adjust the lattice dynamic by changing the ratio of different anions or by changing the chemical/crystal field environment, will open a new route toward the design of more Li superionic conductors.

2.5. Cation Order−Disorder and Blocking Effect

The same system and anion stack sublattice can include a large variation or disorder in the sites of cations and vacancies, which is referred to as the polymorphism of ionic crystal structure. Cations as well as anions are in continuous motion in the crystal structure at finite temperatures. The crystalline structures are statistically average based on the characterization and refinement of XRD, neutron diffraction, *etc.* Most polymorphic structures originate from the cation order−disordered arrangement induced by different occupation and site positions. This can result in different crystal symmetry, band structure, and affect their physical/chemical properties. The most typical example is the cation-disordered rock-salt typed oxide cathode in lithium-ion batteries,[42] while few reports consider these effects when it comes to SSEs. Typically, specific cation and vacancy arrangements lead to unique Li^+ transport properties. Thus, different cation sublattice structures with the same anion stacking can be achieved by changing the content and arrangement of Li^+, M cation, and vacancies in Li-M-X SSEs, which can help us to further understand and optimize the Li^+ transport pathway and hopping effects. Although the function of the cation order−disorder effect in metal halide electrolyte has not been discussed much, there are still many interesting phenomena. Figure 3 reveals some of the reported Li_3MCl_6 structures and the corresponding cation occupation and positions. Wolfgang et al.[24] reported that in some Li_3MCl_6 (M = Y, Er) SSEs, the M^{3+}/vacancies disorder strongly benefits the transport properties. For example, some M_2 atoms in the Li_3MCl_6 (M = Y, Er) structure (Figure 3b), which is occupied the Wyckoff 2d position, can be swapped to the M_3 position. This M_2-M_3 swapping leads to a significant change of the distorted local structure and Li-ion migration barrier. High M_2-M_3 disorder in the structure is beneficial for ionic transport. The RT ionic conductivity of Li_3ErCl_6 compounds with different M_2-M_3 disorders can range from 0.17 to 3.1 × 10^{-4} S cm^{-1}.

https://dx.doi.org/10.1021/acs.accounts.0c00762
Acc. Chem. Res. 2021, 54, 1023−1033

Moreover, the occupation of M cations in the structure will also result in a Coulombic repulsion to Li^+ migration. Based on the theoretical calculation, the Li^+ migration pathways in tetrahedral interstitial sites adjacent to the M cation are blocked. This blocking effect not only reduces the migration efficiency of Li^+ but also distorts the diffusive channels.[1,15] In the ccp-M structure, the Li^+ conducting paths are connected via tetrahedral interstitial sites in all three directions (Figure 4a−c). Therefore, the position and content of the M cation will become a very important factor in the ionic conduction process. Recently, we synthesized a series of Li_xScCl_{3+x} SSEs ($2.5 < x < 4$) with the fast Li^+ conductivity up to 3.02×10^{-3} S cm^{-1}.[1] All Li_xScCl_{3+x} SSEs exhibit a similar monoclinic structure of Li_3ScCl_6 (Figure 4d−g). The only difference is their configurational variability and the occupation of Sc^{3+}, Li^+, and vacancies in the octahedral interstice of Cl^-. Correspondingly, the optimization of vacancies and cations content in the structure can be adjusted by changing the x value. By analyzing the Li^+ density probability of all Li_xScCl_{3+x}, no signal can be found at the tetrahedral site neighboring the Sc site at ∼2.3 Å (Figure 4i). Thus, the tetrahedral interstitial sites adjacent to Sc^{3+} are blocked, which is shown as blue sites in Figure 4h. This blocking effect would distort the diffusion channels of Li^+ (as shown in Figure 4d−g) and result in different Li^+ mobility kinetics. When increasing the x value in Li_xScCl_{3+x}, the Li^+ carrier concentration will be increased, while the opposite trend is observed for the Sc blocking effect and the total vacancy concentration for hopping within the structure. A balance is needed to achieve a structure with appropriate Li^+ carrier concentration and vacancy concentration for Li^+ diffusion as well as continuous diffusion channels. The conduction of ions in solids is a complex physical phenomenon and is affected by many factors. Without a comprehensive understanding of the mechanisms in these ion transport processes, the rational design of new fast ionic conductors is not possible.

3. ENVIRONMENTAL STABILITY AND DEGRADATION CHEMISTRY

Other than high ionic conductivity, other attributes such as environmental stability and the air/humidity tolerance of metal halide SSEs have recently gained significant interest.[2,3,43] Here, we focus on the chemical properties of Li-M-Cl to reveal the environmental stability. The oxidation potential of Cl^- is much higher than O^{2-}, which suggests that O_2 from air cannot oxidize the Cl^- anion in an ambient environment. At the same time, most of the cations in the metal halide SSEs exist in a high valence state. Thus, it is reasonable to assume that most metal halide SSEs are stable in dry air. Moreover, based on the theoretical calculations, most ternary lithium chlorides Li-M-Cl, except for Be^{2+}, show positive hydrolysis reaction energies, which means Li-M-Cl is generally stable against moisture (Figure 5a).[43] The moisture stability for chlorides is much less of an issue when compared to sulfide electrolytes. However, experimentally, most of the Li-M-Cl SSEs suffer from irreversible chemical degradation when exposed to a humid atmosphere. Until now, only Li_3InCl_6 can achieve a reversible ionic conductivity after being exposed to humidity and reheated.[2,16] It is believed that the chemical degradation process when exposed to humidity is very different from that of sulfide electrolytes. Thus, deciphering the degradation process in halide SSEs is of paramount importance. Figure 5b reveals the degradation of ionic conductivity in Li_3YCl_6 and Li_3InCl_6 when exposed to humidity.[2,3] It can be seen that the reduction of ionic conductivity of Li_3YCl_6 is much higher than that of Li_3InCl_6. After reheating, Li_3InCl_6 can be recover over 92% of its initial ionic conductivity, while for Li_3YCl_6, a value of only 0.8% of the pristine ionic conductivity can be retained (Figure 5c,d).

To obtain a clearer picture of the degradation process of Li_3InCl_6 exposed to air, we tracked the chemistry and structure of Li_3InCl_6 during air exposure by using *in situ* and operando synchrotron X-ray analytical techniques.[44] Li_3InCl_6 is hydrophilic, leading to the absorption of moisture to form a hydrate, $Li_3InCl_6{\cdot}xH_2O$. The $Li_3InCl_6{\cdot}xH_2O$ can be dehydrated to products Li_3InCl_6, and then the ionic conductivity can be recovered after a reheating at 200 °C under vacuum conditions. The reversible interconversion between anhydrous and hydrated forms is the reason why Li_3InCl_6 has a high tolerance to water. As the absorption of moisture continues to increase, $Li_3InCl_6{\cdot}xH_2O$ will be dissolved into the water to form a Li_3InCl_6 saturated solution. The pH of Li_3InCl_6 saturated solution is around 4, which suggests a slight hydrolysis process. A small amount of white precipitate such as In_2O_3 will form if the Li_3InCl_6 saturated solution is left standing in ambient air for too long (greater than 24 h). This might be the reason why there's a small irreversible loss of 8% of ionic conductivity between pristine Li_3InCl_6 and the Li_3InCl_6 SSE with long air-exposure time followed by a reheating process. In the dry room environment, the Li_3InCl_6 SSE can be stored and used for more than 1 week without significant reduction in ionic conductivity. However, for Li_3YCl_6, the ionic conductivity cannot be retained even in low humidity environments and will change to $YCl_3{\cdot}6H_2O$ and $LiCl{\cdot}H_2O$ after exposure to air with 3−5% humidity for 12 h.[3] Moreover, Li_3YCl_6 cannot be reformed after reheating the humidity exposed sample in vacuum or inert atmosphere. The resulting product is LiCl and YOCl instead, suggesting a serious hydrolysis reaction process (Figure 5e). Based on the different degradation processes between Li_3InCl_6 and Li_3YCl_6, we further studied the effect of M cations In^{3+} and Y^{3+} and demonstrated the feasibility of increasing the humidity tolerance of $Li_3Y_{1-x}In_xCl_6$ ($0 \le x < 1$) by optimizing the chemical properties via In^{3+} substitution of Y^{3+}.[3] The function of the M cation in Li_3MX_6 was clarified, and the humidity tolerance is highly improved when the In^{3+} content is high enough to form hydrated intermediates, as shown in Figure 5d,e. If we want to achieve metal halide SSEs with high air/humidity tolerance, we need to understand the water absorption and hydrolysis process of the metal halide SSEs. The high humidity tolerance of metal halide SSEs originates from the formation of hydrated intermediates rather than separated hydrated phases.

4. ELECTRODE PROCESSING AND ALL-SOLID-STATE BATTERIES

An ideal SSE should exhibit high ionic conductivity and interfacial compatibility with both cathode and anode.[5,41] However, there is a trade-off between the ionic conductivity and oxidation/reduction stability, which deviates from the ideal SSE.[45] Compared to sulfide and oxide SSEs, switching the anion chemistry from O^{2-} and S^{2-} to halogens such as F^- and Cl^- leads to lattice anions which are more difficult to oxidize. Therefore, metal chloride and fluoride SSEs can achieve high stability toward oxide cathodes. The stable cycling of $LiCoO_2$ and $LiNi_{0.8}Mn_{0.1}Co_{0.1}O_2$, *etc.* oxide cathodes without any

https://dx.doi.org/10.1021/acs.accounts.0c00762
Acc. Chem. Res. 2021, 54, 1023−1033

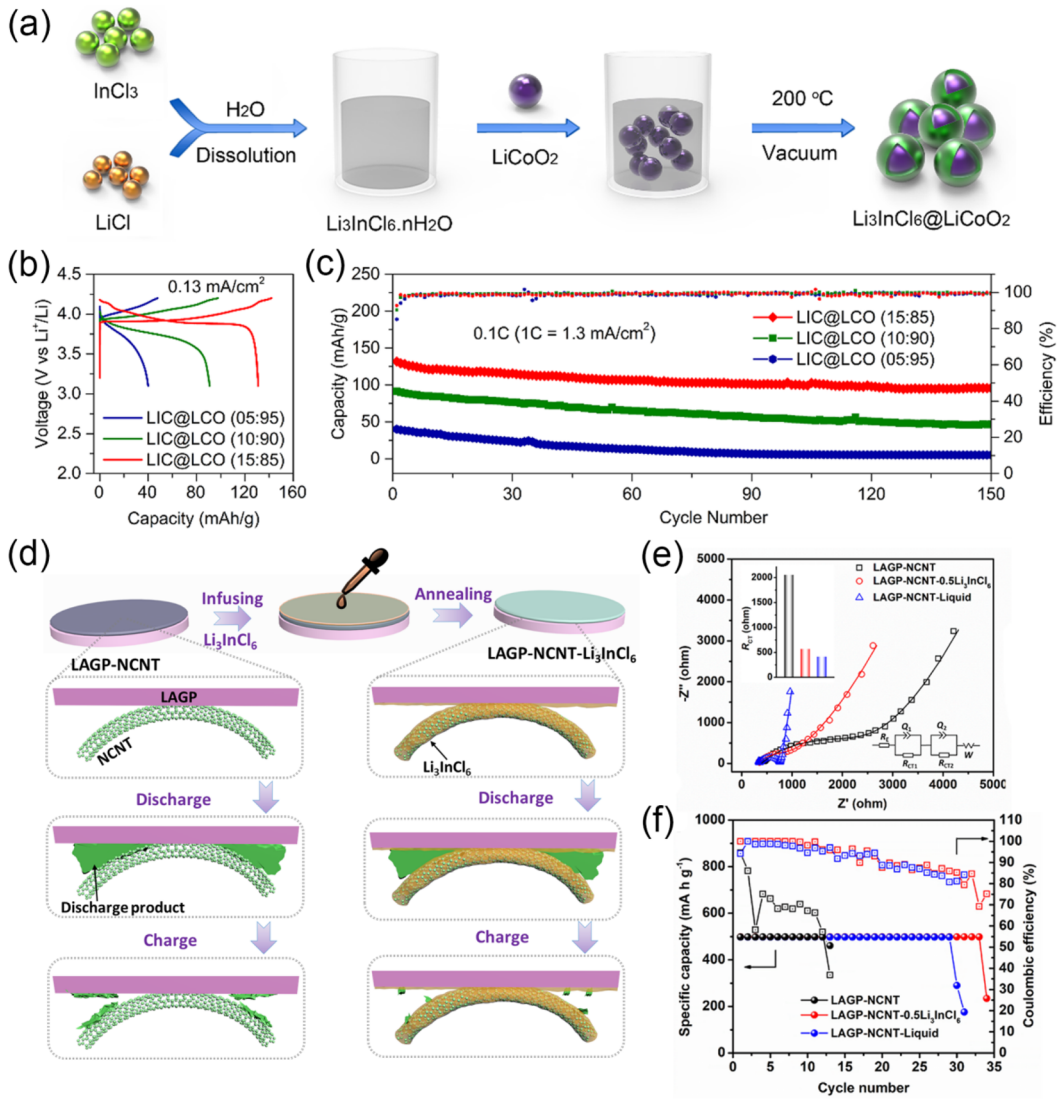

Figure 6. (a) Illustration of the *in situ* synthesis of Li_3InCl_6 on $LiCoO_2$ (LIC@LCO), (b) initial charge/discharge curves of LIC@LCO and (c) corresponding cycling stability, (d) illustration of the synthesis process for the LAGP-NCNT-Li_3InCl_6 air electrode and the effect of Li_3InCl_6 modifier on the decomposition of discharge products, (e) Nyquist plots, and (f) cycling performance of the Li−O_2 batteries with LAGP-NCNT, LAGP-NCNT-0.5Li_3InCl_6, and LAGP-NCNT-liquid air electrodes, respectively. Panels a−c are reproduced with permission from ref 46. Copyright 2020 Elsevier Ltd. Panels d−f reproduced with permission from ref 47. Copyright 2020 Elsevier Ltd.

protection layer can be achieved with the Li-M-Cl electrolytes, which cannot be realized in sulfide electrolyte.[1,2,15,18] Moreover, Li_3InCl_6 SSEs possess the intrinsic advantage of a water-mediated synthesis process, which leads to several advanced potential applications.[2] First, the technique allows for large-scale and easy fabrication of Li_3InCl_6. Our group can achieve more than 100 g sample batches in the lab. Currently, in collaboration with an industrial partner, the scale-up process of Li_3InCl_6 up to the kilogram scale has been successfully achieved. Furthermore, the synthesis is not limited to only anhydrous $InCl_3$ precursors and cheaper hydrated indium chlorides such as $InCl_3{\cdot}4H_2O$; many other kinds of indium compounds such as $In_2(CO_3)_3$, In_2O_3, and $In(OH)_3$ may be used. Second, the water-mediated synthesis process of Li_3InCl_6 enables the application of conformal coatings on cathode materials with ease (Figure 6a). Our group reported an *in situ* interfacial growth of Li_3InCl_6 on $LiCoO_2$ by the water-mediated synthesis process.[46] Owing to the strong interfacial interactions, excellent interfacial compatibility between $LiCoO_2$ and Li_3InCl_6, as well as high interfacial ionic conductivity, $LiCoO_2$ with 15 wt % Li_3InCl_6 coating exhibits a high initial capacity of 131.7 mAh g^{-1} at 0.1 C (1 C = 1.3 mA cm^{-2}) and can be operated up to 4 C at RT (Figure 6b). This interfacial growth process resulted in a uniform coating, which not only reduced the SSE content in the cathode layer but also improved the kinetics of the Li ion transfer. Moreover, stable cycling is achieved with a capacity retention of 90.3 mAh g^{-1} after 200 cycles (Figure 6c). In addition, the water-mediated synthesis process can be further modified as an infiltration process to improve the interfacial contact between two different solid state particles, such as $Li_{1.5}Al_{0.5}Ge_{1.5}(PO_4)_3$ (LAGP) electrolyte and nitrogen-doped carbon nanotube (NCNT) electrodes in Li−O_2 ASSLBs (Figure 6d−f).[47] The resistance between LAGP and NCNT with the infiltration process is comparable to the cells that rely on liquid electrolytes wetting. Moreover, the cycling performance is superior to that of the battery using liquid electrolyte. Metal chloride SSEs are very effective considering their high ionic

https://dx.doi.org/10.1021/acs.accounts.0c00762
Acc. Chem. Res. 2021, 54, 1023−1033

conductivity, low toxicity, and ease of processability. Furthermore, they are stable in dry air and do not require an additional protective coating layer when used in combination with certain oxide cathodes. The main disadvantage of these metal halide SSEs is the low reduction stability due to the electrochemical reduction of metal cations, which prevents the use of Li and graphite anodes.

5. OUTLOOK AND PERSPECTIVE

Metal halide superionic conductors have generated significant interest in the field of ASSLBs. Our group has investigated several novel halide SSEs with RT ionic conductivities higher than 1×10^{-3} S cm^{-1} such as Li_3InCl_6, Li_xScCl_{3+x}, $Li_3Y_{1-x}In_xCl_6$, and Li_3YBr_6, *etc.* In terms of condensed matter physics and chemistry via structural design and Li transport mechanism analysis, there is a great opportunity to push these exciting halide SSEs forward to meet the multiple requirements for energy storage in ASSLBs. We believe a deeper understanding of the Li^+ transport is required to optimize the structure and achieve higher conductivity. Moreover, we proposed and investigated the air/humidity tolerance and degradation chemistry of Li_3InCl_6 electrolyte, which is the only metal halide superionic conductors that can be synthesized in water. The water-mediated synthesis process can be further modified as an *in situ* interfacial growth or infiltration process to improve the interfacial contact between two different solid-state particles such as the cathode particles and SSEs. Currently, metal halide SSEs with higher ionic conductivity (over 1×10^{-2} S cm^{-1}), better environmental/electrochemical stability (especially stable with anode materials such as Li metal), and lower cost are still lacking and need to be developed. Furthermore, factors such as control over the thickness of the metal halide SSEs layer as well as the large scale preparing process should be carried out to achieve practical application in pouch cells. We expect that the development of metal halide SSEs with high ionic conductivity and chemical stability will lead to further understanding of their mechanism and guide new SSE design.

AUTHOR INFORMATION

Corresponding Author

Xueliang Sun − *Department of Mechanical & Materials Engineering, University of Western Ontario, London, Ontario N6A 5B9, Canada;* orcid.org/0000-0003-0374-1245; Email: xsun9@uwo.ca

Authors

Jianwen Liang − *Department of Mechanical & Materials Engineering, University of Western Ontario, London, Ontario N6A 5B9, Canada*

Xiaona Li − *Department of Mechanical & Materials Engineering, University of Western Ontario, London, Ontario N6A 5B9, Canada*

Keegan R. Adair − *Department of Mechanical & Materials Engineering, University of Western Ontario, London, Ontario N6A 5B9, Canada*

Complete contact information is available at: https://pubs.acs.org/10.1021/acs.accounts.0c00762

Notes

The authors declare no competing financial interest.

Biographies

Jianwen Liang is a Mitacs Postdoc Fellow in Prof. Xueliang (Andy) Sun's Group at the University of Western Ontario, Canada. He received his Ph.D. degree in Inorganic Chemistry from the University of Science and Technology of China in 2015. He joined Prof. Sun's group in 2017, and his current research interests include sulfide and halide solid electrolytes as well as all-solid-state Li/Li-ion batteries.

Xiaona Li is a Mitacs Postdoc Fellow in Prof. Xueliang (Andy) Sun's Group at the University of Western Ontario, Canada. She received her Ph.D. degree in Inorganic Chemistry in 2015 from the University of Science and Technology of China. She joined Prof. Sun's group in 2017, and her current research interests focus on the synthesis of sulfide and halide solid electrolytes as well as all-solid-state lithium batteries.

Keegan R. Adair received his B.Sc. in Chemistry from the University of British Columbia in 2016. He is currently a Ph.D. candidate in Prof. Xueliang (Andy) Sun's Group at the University of Western Ontario, Canada. Keegan has previous experience in the battery industry through internships at companies including E-One Moli Energy, and General Motors R&D. His research interests include the design of advanced Li metal anodes and nanoscale interfacial coatings for battery applications.

Xueliang Sun is a Canada Research Chair in Development of Nanomaterials for Clean Energy, Fellow of the Royal Society of Canada, and Canadian Academy of Engineering and Full Professor at the University of Western Ontario, Canada. Dr. Sun received his Ph.D. in Materials Chemistry in 1999 from the University of Manchester, U.K., which he followed up by working as a postdoctoral fellow at the University of British Columbia, Canada, and as a Research Associate at L'Institut National de la Recherche Scientifique (INRS), Canada. His current research interests are focused on advanced materials for electrochemical energy storage and conversion, including solid-state batteries, interface and solid state electrolytes, and electrocatalysts.

ACKNOWLEDGMENTS

This research was supported by the Natural Sciences and Engineering Research Council of Canada (NSERC), the Canada Research Chair Program (CRC), the Canada Foundation for Innovation (CFI), the Ontario Research Fund, a Canada MITACS fellowship, and the University of Western Ontario.

REFERENCES

(1) Liang, J.; Li, X.; Wang, S.; Adair, K. R.; Li, W.; Zhao, Y.; Wang, C.; Hu, Y.; Zhang, L.; Zhao, S.; Lu, S.; Huang, H.; Li, R.; Mo, Y.; Sun, X. Site-occupation-tuned Superionic Li_xScCl_{3+x} halide solid electrolytes for all-solid-state batteries. *J. Am. Chem. Soc.* **2020**, *142*, 7012−7022.

(2) Li, X.; Liang, J.; Chen, N.; Luo, J.; Adair, K. R.; Wang, C.; Banis, M. N.; Sham, T. K.; Zhang, L.; Zhao, S.; Lu, S.; Huang, H.; Li, R.; Sun, X. Water-mediated synthesis of a superionic halide solid electrolyte. *Angew. Chem., Int. Ed.* **2019**, *58*, 16427−16432.

(3) Li, X.; Liang, J.; Adair, K. R.; Li, J.; Li, W.; Zhao, F.; Hu, Y.; Sham, T. K.; Zhang, L.; Zhao, S.; Lu, S.; Huang, H.; Li, R.; Chen, N.; Sun, X. Origin of superionic $Li_3Y_{1-x}In_xCl_6$ halide solid electrolytes with high humidity tolerance. *Nano Lett.* **2020**, *20*, 4384−4392.

(4) Bachman, J. C.; Muy, S.; Grimaud, A.; Chang, H.-H.; Pour, N.; Lux, S. F.; Paschos, O.; Maglia, F.; Lupart, S.; Lamp, P.; Giordano, L.; Shao-Horn, Y. Inorganic solid-state electrolytes for lithium batteries: mechanisms and properties governing ion conduction. *Chem. Rev.* **2016**, *116*, 140−162.

(5) Banerjee, A.; Wang, X.; Fang, C.; Wu, E. A.; Meng, Y. S. Interfaces and Interphases in All-Solid-State Batteries with Inorganic Solid Electrolytes. *Chem. Rev.* **2020**, *120*, 6878−6933.
(6) Zhang, Z.; Shao, Y.; Lotsch, B.; Hu, Y.-S.; Li, H.; Janek, J.; Nazar, L. F.; Nan, C.-W.; Maier, J.; Armand, M.; Chen, L. New horizons for inorganic solid state ion conductors. *Energy Environ. Sci.* **2018**, *11*, 1945−1976.
(7) Li, X.; liang, J.; Yang, X.; Adair, K.; Wang, C.; Zhao, F.; Sun, X. Progress and perspectives of halide-based lithium conductors for all-solid-state batteries. *Energy Environ. Sci.* **2020**, *13*, 1429−1461.
(8) Xu, L.; Li, J.; Deng, W.; Shuai, H.; Li, S.; Xu, Z.; Li, J.; Hou, H.; Peng, H.; Zou, G.; Ji, X. garnet solid electrolyte for advanced all-solid-state Li batteries. *Adv. Energy Mater.* **2021**, *11*, 2000648.
(9) Wang, S.; Bai, Q.; Nolan, A. M.; Liu, Y.; Gong, S.; Sun, Q.; Mo, Y. Lithium chlorides and bromides as promising solid-state chemistries for fast ion conductors with good electrochemical stability. *Angew. Chem., Int. Ed.* **2019**, *58*, 8039−8043.
(10) Plichta, E.; Behl, W.; Vujic, D.; Chang, W.; Schleich, D. The Rechargeable $Li_xTiS_2/LiAlCl_4/Li_{1-x}CoO_2$ solid-state cell. *J. Electrochem. Soc.* **1992**, *139*, 1509.
(11) Weppner, W.; Huggins, R. A. Thermodynamic and phase equilibrium studies of the fast solid ionic conductor $LiAlCl_4$. *Solid State Ionics* **1980**, *1*, 3−14.
(12) Spector, J.; Villeneuve, G.; Hanebali, L.; Cros, C. NMR Investigations of the Li^+ ion mobility in the double chlorides Li_2MgCl_4 and $LiMgCl_3$. *Mater. Lett.* **1982**, *1*, 43−48.
(13) Catlow, C. R. A.; Wolf, M. A molecular-dynamics study of ion transport in lithium magnesium chloride solid electrolytes. *Proc. R. Soc. London Math. Phys. Sci.* **1987**, *413*, 201−224.
(14) Tomita, Y.; Fuji-i, A.; Ohki, H.; Yamada, K.; Okuda, T. New lithium ion conductor Li_3InBr_6 studied by ^7Li NMR. *Chem. Lett.* **1998**, *27*, 223−224.
(15) Asano, T.; Sakai, A.; Ouchi, S.; Sakaida, M.; Miyazaki, A.; Hasegawa, S. Solid halide electrolytes with high lithium-ion conductivity for application in 4 V class bulk-type all-solid-state batteries. *Adv. Mater.* **2018**, *30*, 1803075.
(16) Li, X.; Liang, J.; Luo, J.; Norouzi Banis, M.; Wang, C.; Li, W.; Deng, S.; Yu, C.; Zhao, F.; Hu, Y.; Sham, T. K.; Zhang, L.; Zhao, S.; Lu, S.; Huang, H.; Li, R.; Adair, K. R.; Sun, X. Air-stable Li_3InCl_6 electrolyte with high voltage compatibility for all-solid-state batteries. *Energy Environ. Sci.* **2019**, *12*, 2665−2671.
(17) Park, K. H.; Kaup, K.; Assoud, A.; Zhang, Q.; Wu, X.; Nazar, L. F. High-voltage superionic halide solid electrolytes for all-solid-state Li-ion batteries. *ACS Energy Lett.* **2020**, *5*, 533−539.
(18) Zhou, L.; Kwok, C. Y.; Shyamsunder, A.; Zhang, Q.; Wu, X.; Nazar, L. A new halospinel superionic conductor for high-voltage all solid state lithium batteries. *Energy Environ. Sci.* **2020**, *13*, 2056−2063.
(19) Oi, T.; Miyauchi, K. Amorphous thin film ionic conductors of $mLiF\text{-}nAlF_3$. *Mater. Res. Bull.* **1981**, *16*, 1281−1289.
(20) Feinauer, M.; Euchner, H.; Fichtner, M.; Reddy, M. A. Unlocking the Potential of Fluoride-based Solid Electrolytes for Solid-State Lithium Batteries. *ACS Appl. Energy Mater.* **2019**, *2*, 7196−7203.
(21) Oi, T. Ionic conductivity of LiF thin films containing Di-or trivalent metal fluorides. *Mater. Res. Bull.* **1984**, *19*, 451−457.
(22) Yu, C.; Li, Y.; Adair, K. R.; Li, W.; Goubitz, K.; Zhao, Y.; Willans, M. J.; Thijs, M. A.; Wang, C.; Zhao, F. Tuning ionic conductivity and electrode compatibility of Li_3YBr_6 for high-performance all solid-state Li batteries. *Nano Energy* **2020**, *77*, 105097.
(23) Schlem, R.; Bernges, T.; Li, C.; Kraft, M. A.; Minafra, N.; Zeier, W. G. Lattice Dynamical Approach for Finding the Lithium Superionic Conductor Li_3ErI_6. *ACS Appl. Energy Mater.* **2020**, *3*, 3684−3691.
(24) Schlem, R.; Muy, S.; Prinz, N.; Banik, A.; Shao-Horn, Y.; Zobel, M.; Zeier, W. G. Mechanochemical Synthesis: A tool to tune cation site disorder and ionic transport properties of Li_3MCl_6 (M= Y, Er) superionic conductors. *Adv. Energy Mater.* **2020**, *10*, 1903719.
(25) Steiner, H. J.; Lutz, H. Neue schnelle ionenleiter vom typ $M^I_3M^{III}Cl_6$ (M^I= Li, Na, Ag; M^{III}= In, Y). *Z. Anorg. Allg. Chem.* **1992**, *613*, 26−30.
(26) Stallworth, P.; Fontanella, J.; Wintersgill, M.; Scheidler, C. D.; Immel, J. J.; Greenbaum, S.; Gozdz, A. NMR, DSC and high pressure electrical conductivity studies of liquid and hybrid electrolytes. *J. Power Sources* **1999**, *81*, 739−747.
(27) Kamaya, N.; Homma, K.; Yamakawa, Y.; Hirayama, M.; Kanno, R.; Yonemura, M.; Kamiyama, T.; Kato, Y.; Hama, S.; Kawamoto, K.; Mitsui, A. A lithium superionic conductor. *Nat. Mater.* **2011**, *10*, 682−686.
(28) Kanno, R.; Takeda, Y.; Takada, K.; Yamamoto, O. Ionic Conductivity and phase transition of the spinel system $Li_{2-2x}M_{1+x}Cl_4$ (M= Mg, Mn, Cd). *J. Electrochem. Soc.* **1984**, *131*, 469.
(29) Yu, X.; Bates, J. B.; Jellison, G. E., Jr; Hart, F. X. A stable thin-film lithium electrolyte: lithium phosphorus oxynitride. *J. Electrochem. Soc.* **1997**, *144*, 524.
(30) Rettenwander, D.; Redhammer, G.; Preishuber-Pflugl, F.; Cheng, L.; Miara, L.; Wagner, R.; Welzl, A.; Suard, E.; Doeff, M. M.; Wilkening, M.; Fleig, J.; Amthauer, G. Structural and electrochemical consequences of Al and Ga cosubstitution in $Li_7La_3Zr_2O_{12}$ solid electrolytes. *Chem. Mater.* **2016**, *28*, 2384−2392.
(31) Shannon, R. D. Revised effective ionic radii and systematic studies of interatomic distances in halides and chalcogenides. *Acta Crystallogr., Sect. A: Cryst. Phys., Diffr., Theor. Gen. Crystallogr.* **1976**, *32*, 751−767.
(32) Schmitt, R.; Nenning, A.; Kraynis, O.; Korobko, R.; Frenkel, A. I.; Lubomirsky, I.; Haile, S. M.; Rupp, J. L. M. A review of defect structure and chemistry in ceria and its solid solutions. *Chem. Soc. Rev.* **2020**, *49*, 554−592.
(33) Van der Ven, A.; Bhattacharya, J.; Belak, A. A. Understanding Li diffusion in Li-intercalation compounds. *Acc. Chem. Res.* **2013**, *46*, 1216−1225.
(34) Liu, Y.; Wang, S.; Nolan, A. M.; Ling, C.; Mo, Y. Tailoring the Cation Lattice for Chloride Lithium-Ion Conductors. *Adv. Energy Mater.* **2020**, *10*, 2002356.
(35) Rice, M.; Roth, W. Ionic transport in super ionic conductors: a theoretical model. *J. Solid State Chem.* **1972**, *4*, 294−310.
(36) Xu, Z.; Chen, X.; Liu, K.; Chen, R.; Zeng, X.; Zhu, H. Influence of anion charge on Li ion diffusion in a new solid-state electrolyte, Li_3LaI_6. *Chem. Mater.* **2019**, *31*, 7425−7433.
(37) Muy, S.; Voss, J.; Schlem, R.; Koerver, R.; Sedlmaier, S. J.; Maglia, F.; Lamp, P.; Zeier, W. G.; Shao-Horn, Y. High-throughput screening of solid-state Li-ion conductors using lattice-dynamics Descriptors. *iScience* **2019**, *16*, 270−282.
(38) Kraft, M. A.; Culver, S. P.; Calderon, M.; Böcher, F.; Krauskopf, T.; Senyshyn, A.; Dietrich, C.; Zevalkink, A.; Janek, J. R.; Zeier, W. G. Influence of lattice polarizability on the ionic conductivity in the lithium superionic argyrodites Li_6PS_5X (X= Cl, Br, I). *J. Am. Chem. Soc.* **2017**, *139*, 10909−10918.
(39) Rice, M. J.; Roth, W. L. Ionic transport in super ionic conductors: a theoretical model. *J. Solid State Chem.* **1972**, *4*, 294−310.
(40) Wakamura, K. Roles of phonon amplitude and low-energy optical phonons on superionic conduction. *Phys. Rev. B: Condens. Matter Mater. Phys.* **1997**, *56*, 11593−11599.
(41) Xiao, Y.; Wang, Y.; Bo, S.-H.; Kim, J. C.; Miara, L. J.; Ceder, G. Understanding interface stability in solid-state batteries. *Nat. Rev. Mater.* **2020**, *5*, 105.
(42) Clément, R. J.; Lun, Z.; Ceder, G. Cation-disordered rocksalt transition metal oxides and oxyfluorides for high energy lithium-ion cathodes. *Energy Environ. Sci.* **2020**, *13*, 345−373.
(43) Zhu, Y.; Mo, Y. Materials design principles for air-stable lithium/sodium solid electrolytes. *Angew. Chem., Int. Ed.* **2020**, *59*, 17472−17476.
(44) Li, W.; Liang, J.; Li, M.; Adair, K. R.; Li, X.; Hu, Y.; Xiao, Q.; Feng, R.; Li, R.; Zhang, L.; Lu, S.; Huang, H.; Zhao, S.; Sham, T. K.; Sun, X. Unraveling the origin of moisture stability of halide solid-state

electrolytes by *in situ* and operando synchrotron X-ray analytical techniques. *Chem. Mater.* **2020**, *32*, 7019−7027.
(45) Manthiram, A.; Yu, X.; Wang, S. Lithium battery chemistries enabled by solid-state electrolytes. *Nat. Rev. Mater.* **2017**, *2*, 16103.
(46) Wang, C.; Liang, J.; Jiang, M.; Li, X.; Mukherjee, S.; Adair, K.; Zheng, M.; Zhao, Y.; Zhao, F.; Zhang, S.; Li, R.; Huang, H.; Zhao, S.; Zhang, L.; Lu, S.; Singh, C. V.; Sun, X. Interface-assisted *in-situ* growth of halide electrolytes eliminating interfacial challenges of all-inorganic solid-state batteries. *Nano Energy* **2020**, *76*, 105015.
(47) Zhao, C.; Liang, J.; Li, X.; Holmes, N.; Wang, C.; Wang, J.; Zhao, F.; Li, S.; Sun, Q.; Yang, X.; Liang, J.; Lin, X.; Li, W.; Li, R.; Zhao, S.; Huang, H.; Zhang, L.; Lu, S.; Sun, X. Halide-based solid-state electrolyte as an interfacial modifier for high performance solid-state Li-O_2 batteries. *Nano Energy* **2020**, *75*, 105036.

https://dx.doi.org/10.1021/acs.accounts.0c00762
Acc. Chem. Res. 2021, 54, 1023−1033